



Sorption and desorption experiments using stable cesium: considerations for radiocesium retention by fresh plant residues in Fukushima forest soils

Takuya Manaka¹ · Shinta Ohashi² · Sumika Ogo³ · Yuichiro Otsuka⁴ · Hitomi Furusawa¹

Received: 1 February 2021 / Accepted: 23 March 2021 / Published online: 17 May 2021
© The Author(s) 2021

Abstract

We conducted sorption experiments with stable cesium (^{133}Cs) solution in different organic matter samples, aiming to understand the sorption of radiocesium (^{134}Cs and ^{137}Cs) in the initial throughfall by fresh plant residues (e.g., needles, wood, and bark from Japanese cedar trees) in the Oi horizon in forests in Fukushima. Among the organic matter samples, bark and wattle tannin sorbed relatively large amounts of Cs, whereas wood and cellulose powder sorbed small amounts. In contrast, samples containing clay minerals showed much higher Cs sorption. We also conducted desorption experiments, and suggested that Cs on the organic matter samples were relatively mobile.

Keywords Fukushima Dai-ichi nuclear power plant accident · Cesium · Forest soils · Organic matter · Sorption and desorption · Vermiculite

Introduction

Following the Fukushima Dai-ichi Nuclear Power Plant accident in March 2011, a large amount of radiocesium, (mainly ^{134}Cs and ^{137}Cs), was released and deposited in forested areas of Fukushima, Japan [1–3]. In the first few years after the accident, most radiocesium was first trapped in the canopy of the evergreen coniferous trees and then gradually transferred in a soluble form via throughfall onto the forest floor, with large spatial variations [4–6]. In the forest soils, mainly the A horizon (the surface mineral horizon mixed

with some humus), clay minerals, such as illite or vermiculite, have adsorption sites for monovalent cations of radiocesium with a significantly strong affinity (e.g., wedge-shaped expanded zones in their interlayer (frayed edge sites; FES) and type II sites) [7–11]. In contrast, organic matter in the O horizon (the surface organic horizon), including leaves/needles, bark, and wood can also sorb radiocesium. Monovalent cations of radiocesium can be electrostatically bound to negatively charged sites on the surface or physically trapped in the complex structures of this organic matter [12, 13]. Generally, radiocesium sorbed on organic matter is relatively mobile because it rapidly migrates downward to the A horizon or is easily taken up by plant roots or microorganisms [6, 14]. However, in the natural environment, various types and degradation degrees of organic matter are frequently mixed with clay minerals derived from soil bioturbation or eolian dust. Indeed, the O horizon is separated into Oi, Oe, and Oa horizons, in the order of decomposition of organic matter. Geological, topographic, and biological conditions can also affect the type and degradation degree of organic matter. In addition, the access of radiocesium to the strong affinity sites of clay minerals can be blocked by humified organic matter [10, 15–18]. These transportation and sorption mechanisms lead to the heterogeneous distribution of radiocesium, complicating estimates of radiocesium cycling in forest ecosystems [13, 19, 20].

✉ Takuya Manaka
manaka@affrc.go.jp

¹ Department of Forest Soils, Forestry and Forest Products Research Institute, 1 Matsunosato, Tsukuba, Ibaraki 305-8687, Japan
² Department of Wood Properties and Processing, Forestry and Forest Products Research Institute, 1 Matsunosato, Tsukuba, Ibaraki 305-8687, Japan
³ Department of Mushroom Science and Forest Microbiology, Forestry and Forest Products Research Institute, 1 Matsunosato, Tsukuba, Ibaraki 305-8687, Japan
⁴ Department of Forest Resource Chemistry, Forestry and Forest Products Research Institute, 1 Matsunosato, Tsukuba, Ibaraki 305-8687, Japan

Our final goal is to demonstrate the heterogeneous distribution of radiocesium in forest soils and to elucidate the role of organic matter in radiocesium cycling in Fukushima forest ecosystems. As a trial, this study focused on fresh and undecomposed plant residues in the Oi horizon in Fukushima evergreen coniferous forests. We conducted simple batch sorption experiments in the laboratory to estimate how much radiocesium in the initial throughfall can be sorbed by individual fresh plant residues. Similar experiments have been conducted in the context of industrial decontamination or the production of soil additive, of which main targets are zeolite or charcoals [21–23]. The sorption characteristics of clay mineral samples or mineral soils in natural environments (mainly agricultural fields) also have been evaluated previously [8–10, 24]. However, to our knowledge, few studies have focused on organic matter in forest ecosystems. Here, we examined fresh plant residue, including the needles, wood, and bark of Japanese cedars (*Cryptomeria japonica*), the most widely planted tree species in Japan, collected in several study sites (e.g., Imamura et al. [25]). In addition, the natural organic compounds, cellulose and tannin, which are the main components of wood and bark, respectively, were tested. Furthermore, we collected the O and A horizon sample from forests in Fukushima. The clay mineral vermiculite was also examined. For this trial, we used stable cesium (^{133}Cs), which has the same chemical characteristics as radiocesium. Although the limit of quantitation of ^{133}Cs by inductively coupled plasma mass spectrometry (ICP-MS) is much higher per mole than that of radiocesium by gamma ray spectrometer, ^{133}Cs is very easy to handle for examining the general sorption characteristics of organic matter samples over a wide concentration range. To examine the mechanisms of Cs sorption, experiments with pH-controlled solutions or with organic matter (cedar needles) mixed with clay minerals (A horizon sample) were also investigated. Finally, we examined the ability of ultrapure water or ammonium acetate solution to desorb Cs, as an analog of the mobility and bioavailability of Cs that was once sorbed on individual fresh plant residues [26].

Materials and methods

Materials

Three fresh plant residues (needles, wood, and bark samples of Japanese cedar trees), two natural organic compounds (cellulose powder and wattle tannin), O and A horizon samples, and a vermiculite standard were used in these experiments. Although the fresh plant residues and O and A horizon samples were collected in different sites, all of these sites were at the mature forest stage of Japanese cedar

plantation in Fukushima and the neighboring prefecture, Ibaraki. The sampling surveys were conducted in mainly summer.

The needle litter sample was collected before transferred onto the forest floor by using litter traps set in a Japanese cedar plantation in Tsukuba Forest Experimental Watershed of Forestry and Forest Products Research Institute, Ibaraki, Japan, from July to October 2013 (stand age: 60 years in 2013). Details of this plantation are described in Inagaki et al. [27].

The wood sample was collected in August 2014 from a Japanese cedar plantation in Kawauchi Village, Fukushima, Japan (stand age: 46 years in 2014); details are described as KU1-S in Imamura et al. [25]. We sampled wood disks at breast height and divided these into sapwood and heartwood samples. In this study, we utilized only sapwood for the experiments, because most of the fallen wood in the Oi horizon is assumed to be sapwood, not heartwood.

The bark sample was collected in August 2014 from a Japanese cedar plantation in Otama Village, Fukushima, Japan (stand age: 45 years in 2014; OT-S in Imamura et al. [25]). We used the whole bark and did not divide it into outer and inner bark.

Cellulose powder (SolkaFloc #40) was purchased from Imazu Chemical Co. Ltd. (Chiyoda City, Tokyo, Japan).

Wattle tannin powder, a major manufactural condensed tannin, was extracted from the bark of *Acacia mearnsii*. Our sample was obtained from Sumitomo Dainippon Pharma Co., Ltd., Osaka City, Osaka, Japan (current affiliation: DSP Gokyo Food & Chemical Co., Ltd, Osaka City, Osaka, Japan). Because of a limited sample mass, some subsequent experiments were not conducted for this sample.

The O and A horizon samples were collected in August 2019 in another Japanese cedar plantation in Kawauchi Village (stand age: 63 years in 2019; KU2-S in Imamura et al. [25]). The forest soils in this site were derived from volcanic ash and classified as Andosols [28]. The clay fractions of the A horizon were mainly composed of vermiculite, with a small amount of quartz, kaolinite, and chlorite [29]. The O horizon sample (including the Oi, Oe, and Oa horizons) was collected from a 25 cm × 25 cm quadrat. The A horizon samples were collected from the 5–10 cm depth after removing the O horizon, using a 475 mL cylinder (95 cm² cross-sectional area × 5 cm length). Details of these sampling methods are given in Ikeda et al. [30].

We used the vermiculite standard sample from Nichika Inc. (Kyoto City, Kyoto, Japan). This sample was originally collected in Asakawa Town, Fukushima, and crushed to a diameter of < 50 μm.

After sampling, the needle, wood, and bark samples were oven-dried at 75 °C, and the O and A horizon samples were air-dried. Prior to experiments, these samples were well-mixed and stored at room temperature in the laboratory.

The needle, wood, bark, and O horizon samples were powdered by a hi-speed vibrating sample mill (TI-200; CMT Co. Ltd., Iwaki City, Fukushima, Japan). The wattle tannin was insolubilized with formaldehyde, which is used as a cross-linking agent [31]. After this reaction, the sample was thoroughly washed with ultrapure water, freeze-dried, and homogenized.

The particle size of each sample (except for the A horizon sample) was measured via a laser diffraction particle size analyzer (SALD-2300; Shimadzu Corporation, Kyoto City, Kyoto, Japan). The particle size distribution for the A horizon sample was already analyzed through a pipette method and reported by Forestry Agency of Japan [29]; the percentage of clay (<0.002 mm), silt (0.002–0.02 mm), fine sand (0.02–0.2 mm), and coarse sand (0.2–2 mm) was 23%, 42%, 26%, and 9%, respectively.

The concentration of Cs in each pre-Cs-sorption sample (Q_{0-A} , unit: mol kg⁻¹) was measured by the wet ashing method. An aliquot of each sample (approximately 0.1 g) was digested with nitric acid and hydrogen peroxide in a heating block system. We also used hydrofluoric acid to digest the A horizon sample and vermiculite. The Cs concentration of the solution was measured via ICP-MS (Agilent7700X; Agilent Technologies, Santa Clara, CA, USA; iCAP Qc, Thermo Fisher Scientific, Waltham, MA, USA). We used the chemical reagent of CsCl (FUJIFILM Wako Pure Chemical Corporation, Osaka City, Osaka, Japan) for the calibration standard as well as the following experiments. Scandium, yttrium, and cerium (AccuStandard, New Haven, CT, USA) were added and used as internal standards. Analytical errors and limits of quantitation for ICP-MS measurements were approximately 5% and 3×10^{-10} mol kg⁻¹, respectively, which were estimated from repeated measurements of our representative samples in the following experiments and the calibration blank.

We also measured the ash content as follows: an aliquot of each sample (approximately 0.5 g) was oven-dried at 105 °C and then burned in a muffle furnace at 500 °C for 4 h [32].

Experiment A: Cesium sorption experiments

Sorption experiments of Cs were conducted in the following simple settings to estimate how much radiocesium in the initial throughfall after the accident can be sorbed by each sample. We used the chemical reagent of CsCl, dissolved in ultrapure water. Each sample (0.50 g) and 10 g of CsCl solution were placed in a centrifuge tube (mixture ratio of 1:20) mixed by a reciprocating shaker at room temperature. Because the sorption of Cs by each sample might be affected by the initial concentration of the CsCl solution [24] and the contact time between the solution and the sample [33], we prepared five Cs concentrations for the initial solution

(C_1 : 1.00×10^{-7} , 1.00×10^{-6} , 1.00×10^{-5} , 1.00×10^{-4} , and 1.00×10^{-3} mol kg⁻¹) and three contact times (2, 24, and 48 h) for each sample. For wattle tannin, we conducted only 24 h shaking. After shaking, the mixtures were immediately centrifuged, and the supernatant solutions were passed through syringe filters (pore size: 0.45 μm). The Cs concentration of the filtrates (C_2 , unit: mol kg⁻¹) was analyzed by ICP-MS (diluted with nitric acid at the time of ICP-MS analysis). These treatments were repeated at least twice for each sample and Cs concentration.

In addition, to evaluate the impact of Cs that is originally included in the samples on this sorption experiment, 0.50 g of each pre-Cs-sorption sample was mixed with 10 g of ultrapure water, shaken for 24 h, centrifuged, and filtered. Then, the Cs concentration of the filtrates was also analyzed.

Experiment A-1: Cesium sorption under controlled pH

Assuming that negatively charged sites (e.g., phenolic hydroxyl or carboxyl groups) on the surface of organic matter is mainly attributed to Cs sorption, the pH in the solution should control Cs sorption by affecting the dissociation of these groups [34, 35]. To test for the impact of pH, we conducted sorption experiments with a pH-controlled CsCl solution on needle, wood, bark, cellulose powder, wattle tannin, and vermiculite samples. We used the pH standard buffer solution for pH 6.86 ($0.025 \text{ mol kg}^{-1} \text{ Na}_2\text{HPO}_4 + 0.025 \text{ mol kg}^{-1} \text{ KH}_2\text{PO}_4$) and for pH 4.01 ($0.05 \text{ mol kg}^{-1} \text{ C}_6\text{H}_4(\text{COOK})(\text{COOH})$) from FUJIFILM Wako Pure Chemical Corporation. For these solutions, we added CsCl for a Cs concentration of 1.00×10^{-5} mol kg⁻¹. The sorption experiments were conducted at a mixture ratio of 1:20 and 24 h shaking at room temperature for these samples. These treatments were repeated twice for each sample and pH condition. Note that the background solution matrices and ion strength of the initial solution in this experiment, which can significantly affect Cs sorption [9, 35], are entirely different from those in Experiment A. Thus, the results of Experiment A-1 cannot be directly compared with those of Experiment A.

We also measured the pH values of these suspending solutions, besides the mixture of ultrapure water and each sample after 24 h shaking, with a pH meter (HM-25R; DKK-TOA Corporation, Shinjuku City, Tokyo, Japan). The ultrapure water pH was also measured for the O and A horizon samples.

Experiment A-2: Cesium sorption for cedar needles with A horizon sample

Both organic matter and clay minerals are admixed in the natural environment of the forest soils, even in the O horizon, and it is almost impossible to distinguish between them.

We prepared a cedar needle sample mixed with A horizon sample at mass ratios of 98:2, 95:5, 90:10, 85:15, 80:20, 70:30, 50:50, and 25:75 to investigate how the incorporation of clay minerals can affect Cs sorption by organic matter. The Cs sorption experiments also were conducted for these mixtures; the mixing ratios of the total mass of the mixture and CsCl solution were the same as those in Experiment A (1:20). Only three levels of Cs concentrations in the initial solution (1.00×10^{-7} , 1.00×10^{-6} , and 1.00×10^{-5} mol kg⁻¹) and shaking at room temperature for 24 h were examined. These treatments were repeated at least twice for each sample and mixing ratio.

Experiment B: Cesium desorption experiments

We conducted desorption experiments using methods modified from Manaka et al. [6] to evaluate the mobility and bioavailability of Cs sorbed by each sample. As a representative setting of Experiment A, Cs was sorbed on each sample with 1.00×10^{-5} mol kg⁻¹ of CsCl solution and 24 h shaking at room temperature. The residue was recovered by suction filtration (pore size: 0.45 μm) and oven-dried at 105 °C. After drying, the residue was mixed thoroughly at room temperature. An aliquot of each residue (approximately 0.5 g) was digested by the wet ashing method for ICP-MS analysis, and total Cs concentrations of the residue (Q_{0-B} , unit: mol kg⁻¹) were obtained. In addition, two aliquots of each residue (0.50 g) were placed into two centrifuge tubes, and 10 g of ultrapure water or ammonium acetate (1 mol kg⁻¹, pH 7.0) was added. The mixture was shaken for 2 h at room temperature and centrifuged. The supernatant solution was passed through syringe filters, and the Cs concentration (C_3 , unit: mol kg⁻¹) was analyzed via ICP-MS. These treatments were repeated at least twice for each sample and desorption solution.

Results and discussion

Cesium sorption on organic matter samples

The median particle diameters were in the same order of magnitude for all our organic matter samples (the needles, wood, bark, cellulose powder, and wattle tannin) (Table 1). The concentration of Cs in each pre-Cs-sorption sample (Q_{0-A}) in Experiment A were also summarized in Table 1: considering the initial concentration of the CsCl solution (C_1 : 1.00×10^{-7} to 1.00×10^{-3} mol kg⁻¹) and the mixing ratios of samples and CsCl solutions in this experiment (1:20), these values were low enough to neglect the impact of innate Cs in the samples for these experiments. Similarly, the Cs concentration of the filtrates after mixing with ultrapure water was negligible, lower than the method quantification limit (3×10^{-9} mol kg⁻¹).

In this experiment, the proportion of Cs sorption (%) was simply calculated by subtracting the Cs concentration of the filtrates (C_2 ; Table 2 in “Appendix”) from C_1 , as given in the following Eq. (1):

$$\text{Proportion of Cs sorption (\%)} = (C_1 - C_2) / C_1 \times 100 \quad (1)$$

As a representative setting of this experiment, Fig. 1 shows the proportion of Cs sorption in $C_1 = 1.00 \times 10^{-5}$ mol kg⁻¹. No obvious trends were observed for different contact times (2, 24, and 48 h), which suggests that the time required to reach equilibrium for Cs sorption may be short. Among the three fresh plant residues, the amount of Cs sorbed by bark (37% for 24 h shaking) was relatively large, followed by needles (29%) and wood (20%). For the two natural organic compounds, the proportion of Cs sorption of cellulose powder (26%) was approximately the same as that of needles and wood, whereas the proportion of wattle tannin (70%) was much higher than that of bark.

Table 1 Median particle diameter, Cs concentration (Q_{0-A}), ash content, and pH (suspended solution with ultrapure water and pH standard buffer solution for pH 6.86 and 4.01, measured after 24 h shaking)

Component	Median particle diameter (μm)	Cs concentration (Q_{0-A}) (mol kg ⁻¹)	Ash content (%)	pH		
				Ultrapure water	Initial pH: 6.86	Initial pH: 4.01
Needles	45	1.9×10^{-7}	5.5	4.90	6.49	4.20
Wood	60	4.0×10^{-8}	0.4	4.43	6.72	4.01
Bark	48	1.6×10^{-7}	2.5	3.26	5.76	3.62
Cellulose powder	74	$< 3.0 \times 10^{-8}$	0.3	5.86	6.85	4.04
Wattle tannin	24	2.5×10^{-7}	0.4	4.86	6.53	4.02
O horizon sample	45	7.1×10^{-7}	4.8	5.28	–	–
A horizon sample	–	1.7×10^{-5}	74.5	5.36	–	–
Vermiculite	18	3.7×10^{-5}	95.8	9.24	6.93	4.77

The ash content was calculated based on oven-dried mass at 105 °C

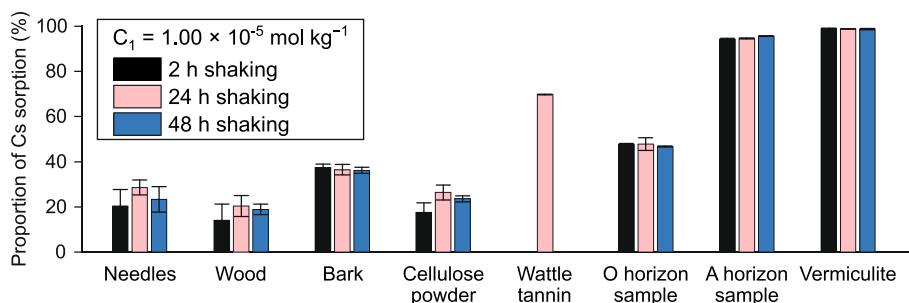


Fig. 1 Bar charts of the proportion (%) of Cs sorption over time in Experiment A. The initial concentration of $C_1 = 1.00 \times 10^{-5} \text{ mol kg}^{-1}$ was used for contact times of: 2 h (black), 24 h (red), and 48 h (blue).

For wattle tannin, we have conducted only 24 h shaking due to a limited supply. The error bars indicate 1 SD. Table 2 in “Appendix” also shows the numerical data

Furthermore, we examined Freundlich isotherm, a major sorption model, to evaluate the impact of different C_1 values on Cs sorption. First, the Cs concentration sorbed on the sample (Q_1 , unit: mol kg^{-1}) was calculated as follows:

$$Q_1 = (C_1 - C_2)M_{\text{solution}}/M_{\text{sample}} \quad (2)$$

where M_{solution} and M_{sample} are the mass of the solution (10 g) and the sample (0.5 g), respectively. The equation for the Freundlich isotherm was described as follows:

$$Q_1 = K_f C_2^{1/n} \quad (3)$$

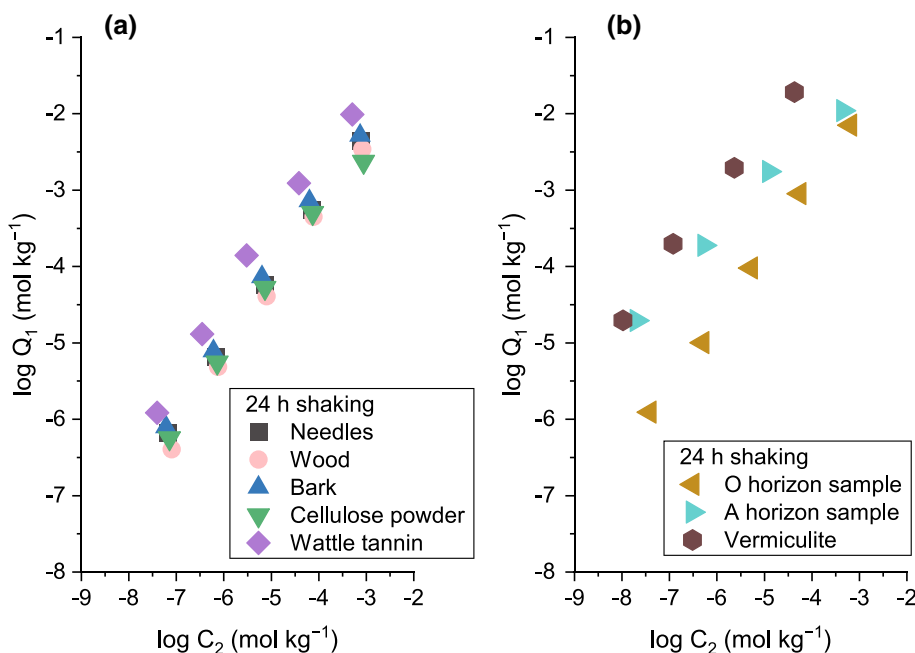
where K_f and $1/n$ are the Freundlich coefficient. This equation can be linearized as

$$\log Q_1 = \log K_f + 1/n \log C_2 \quad (4)$$

Table 3 in “Appendix” summarizes the numerical results of the linear regression. Because no obvious trends were observed for different contact times, we plotted only the results of 24 h shaking, as a representative setting (Fig. 2a). A high coefficient of determination (r^2) in all organic matter samples and contact times, between 0.994 and 1.000, indicated that this model properly describes Cs sorption between the solution and various samples. In all cases in our experiments, $1/n$ values were less than 1, and the relative amount of Cs adsorbed on each sample decreased when the Cs concentration of the solution increased. Note that the Freundlich isotherm is an empirical model, implying the existence of multi-component sorption sites. Each coefficient can be affected by many factors, such as the number of sorption sites and their affinity [36, 37].

As shown for both the proportion of Cs sorption (Fig. 1) and the Freundlich isotherm (Fig. 2a; Tables 2 and 3), the

Fig. 2 Scatter plots of log-transformed Cs concentration sorbed on each sample (Q_1) and log-transformed Cs concentration of the filtrates (C_2), after 24 h shaking in Experiment A: **a** organic matter samples (needles, wood, bark, cellulose powder, and wattle tannin) and **b** samples containing clay minerals (the O and A horizon samples and vermiculite). In “Appendix”, Table 2 shows the numerical data, and Table 3 presents the parameters for linear fitting. Data that were lower than the method quantification limit are not shown in these plots



amount of Cs sorbed by bark and wattle tannin was relatively large among organic matter samples. Tannin, a main component of bark, has abundant phenolic hydroxyl groups. The ortho-dihydroxyl groups in the B-ring (catechol) particularly show a high affinity for multivalent heavy metals, electrostatically adsorbing them, and forming complexes [31, 34]. To evaluate whether this process applies to a monovalent cation of Cs, we conducted sorption experiments with a pH-controlled CsCl solution (Experiment A-1). For wattle tannin, the proportion of Cs sorption increased when the pH of the solution increased (Fig. 3).

A higher pH is expected to stimulate the dissociation of phenolic hydroxyl groups to form negative charges [34], on which a monovalent cation of Cs can adsorb. Similarly, the contribution of carboxyl groups as well as phenolic hydroxyl groups on the electrostatic adsorption of metal cations has been reported for bark samples [38, 39]. Carboxyl groups can work as a strong acid under experimental conditions, showing pH-dependent negative charges [35]. For these reasons, we suggest that pH-dependent negative charges of phenolic hydroxyl or carboxyl groups make an essential contribution to the relatively high sorption of Cs on bark and wattle tannin.

Cedar needles moderately sorbed Cs (Figs. 1 and 2a; Tables 2 and 3). We also observed pH dependence of the proportion of Cs sorption (Fig. 3), suggesting a similar process of Cs sorption as that of bark and wattle tannin. We note that the organic carbon composition of the needles is also complex. Ono et al. [40] reported different signals of aliphatic, aromatic, and carbonyl carbon in different degradation stages by the solid-state ^{13}C CPMAS NMR technique. The contribution of phenolic hydroxyl or carboxyl groups on Cs sorption has been suggested in humic substances [35, 41].

The amount of sorbed Cs by wood and cellulose powder was relatively small (Figs. 1 and 2a; Tables 2 and 3). Unlike other organic matter samples, no difference was observed for the proportion of Cs sorption at different pH values (Fig. 3). Generally, the number of activated negative charges of phenolic hydroxyl or carboxyl groups is much smaller in wood than in bark [38]. The hydroxyl groups of cellulose can only work as weak acids under experimental conditions, showing a low adsorption capacity toward metal [42]. One possible mechanism for pH-independent Cs sorption is the nonspecific physical traps of Cs inside the complex, three-dimensional structure of cellulose, such as microfibrils. Further studies with different methods are required to elucidate these mechanisms.

Cesium sorption on samples containing clay minerals

Compared with the organic matter samples, the Q_{0-A} values were two orders of magnitude higher in vermiculite and the A horizon sample (Table 1), because Cs naturally occurs in the earth's crust and sedimentary rocks [43]. However, the Cs concentration of the filtrates after mixing with ultrapure water was lower than the method quantification limit in these samples (3×10^{-9} mol kg^{-1}). This result indicates a very strong and almost irreversible sorption of Cs in clay minerals [7, 10, 11], and a negligible impact of Cs innately included in these samples. Similar to the organic matter samples, no significant trend of C_2 values at different contact times (2, 24, and 48 h) was observed for these samples (Table 2).

Sorption of Cs on vermiculite also was described in the Freundlich isotherm model ($r^2 = 0.998\text{--}0.999$) (Fig. 2b; Tables 2 and 3). Compared with the organic matter samples, extraordinarily low C_2 values and high Q_1 values suggest that almost all of the Cs in the solution was sorbed by this

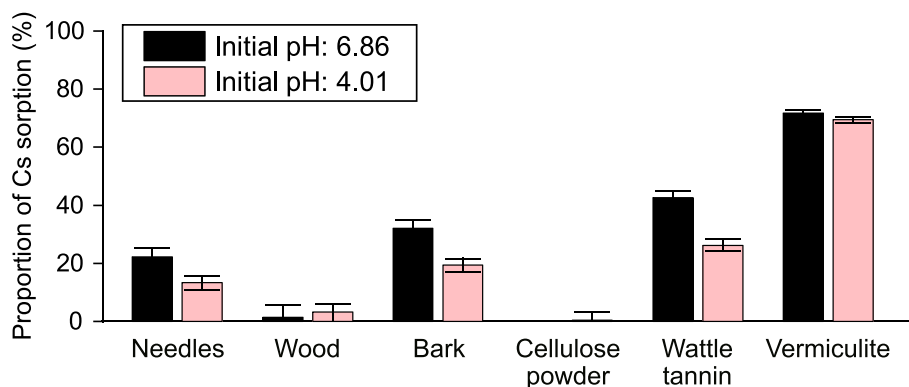


Fig. 3 Bar charts of the proportion (%) of Cs sorption under the pH-controlled condition for needle, wood, bark, cellulose powder, wattle tannin, and vermiculite samples, in Experiment A-1. The initial Cs concentration was 1.00×10^{-5} mol kg^{-1} , and the contact time was

24 h. Black and red bars indicate initial pH values of 6.86 and 4.01, respectively. The error bars indicate 1 SD. Table 1 shows the numerical pH values of the suspended solutions after shaking

sample. Such high sorption has been demonstrated in previous studies [44][44]. According to Bradbury and Baeyens [8], Fan et al. [10], and Fuller et al. [9], in similar concentration ranges of Cs as the C_2 values of our experiments, FES and type II sites are the dominant contributors of Cs adsorption, forming an inner-sphere complex with strong affinity. These adsorption sites may have permanent negative charges derived from isomorphous substitutions in the mineral structure.

In Experiment A-1, we observed a negligible difference of the proportion of Cs sorption with different pH levels in vermiculite (Fig. 3). This result is comparable with the experiments of Fuller et al. [9] in the pH range of 4–7 and with background solution matrices of sodium and potassium, although they also proposed that Cs adsorption to type II sites can be affected by competition with hydrogen ions. We also note that in this sample, the proportion of Cs sorption was relatively lower when C_1 was 1.00×10^{-4} or 1.00×10^{-3} mol kg⁻¹, and $1/n$ values were lower (Tables 2 and 3). This indicates that high-affinity adsorption sites begin to saturate in solutions with high Cs concentrations [8, 9].

The Cs sorption on the A horizon sample showed similar trends as vermiculite, showing significantly low C_2 values and high Q_1 values (Fig. 2b; Tables 2 and 3) compared with organic matter samples and described by the Freundlich isotherm model ($r^2 = 0.988$ – 0.994). The $1/n$ values were lower than those for vermiculite, suggesting near saturation of Cs adsorption sites when C_1 was high. However, the affinity of the sorption site for Cs may be weaker, as discussed with the results of desorption experiments (Experiment B) in the next section.

For the O horizon sample, Cs sorption also was described in the Freundlich isotherm model ($r^2 = 0.999$ – 1.000), and the amount of Cs sorbed by this sample seemed to be higher than most organic matter samples (except for wattle tannin) but lower than the A horizon sample (Figs. 1 and 2; Tables 2 and 3). The O horizon sample comprised various organic matter, including needles or bark at different degradation stages; pH-dependent negative charges such as phenolic hydroxyl or carboxyl groups should contribute to the Cs sorption in this sample. In addition, this sample also contains clay minerals derived from soil bioturbation or eolian dust. Fujii et al. [46] measured the radiocesium interception potential (RIP) by FES in O horizon samples from Kawauchi Village (KU1-S). Their result of 3.6×10^{-2} mol kg⁻¹, which is equivalent to an FES content of 3.6×10^{-5} mol kg⁻¹ (assuming that the selectivity coefficient of trace Cs to K of the FES ($K_{C(Cs-K)}^{FES}$) in RIP measurement is 1000, as shown by Wauters et al. [47]), was sufficiently high to adsorb all Cs in the solution at a C_1 value of 1.00×10^{-7} or 1.00×10^{-6} mol kg⁻¹. The sampling site of Fujii et al. [46] was different from ours (KU2-S), but their findings may be partly applicable to our O horizon sample. The clay minerals

incorporated into our samples may show a higher affinity to Cs than other organic matter, thus increasing the amount of sorbed Cs, although not all Cs in the solution was sorbed, even under C_1 values of 1.00×10^{-7} or 1.00×10^{-6} mol kg⁻¹. We note that some studies also report that organic matter can block Cs from accessing the strong affinity sites of clay minerals [10, 15–18].

The amount of clay minerals incorporated into the O horizon is difficult to quantify. The ash content (Table 1) is a possible analog for this [13, 46], but we note that some ash also can be derived from plant opals or inorganic salts in plant litter. We examined the Cs sorption of needles combined with the A horizon sample to demonstrate to what extent the incorporation of clay minerals can affect Cs sorption by organic matter (Fig. 4). The proportion of Cs sorption increased when the proportion of the A horizon sample mass increased, implying a preferential Cs sorption by clay minerals, which also was suggested by our O horizon sample. Furthermore, C_1 values should significantly affect the proportion of Cs sorption; when C_1 was 1.00×10^{-5} mol kg⁻¹, a positive and nearly linear relationship was observed between the proportion of the A horizon sample mass and Cs sorption (Fig. 4c). In contrast, when C_1 values were smaller, the proportion of Cs sorption drastically increased with even small incorporation of A horizon sample (Fig. 4a, b). Under natural conditions, the maximum amount of ¹³⁷Cs deposition was reported to be 1.55×10^7 Bq m⁻² (equal to 3.53×10^{-8} mol m⁻²), observed at a study site very close to the power plant [48]. Assuming that the mean inventory of the organic matter in the O horizon is 1.4 kg m⁻² [25], this value is much smaller in molar units than the amount of Cs in the solution of our experiments. Thus, our results imply a more essential role of clay minerals in their preferential sorption of radiocesium in the natural condition.

We note that these are trial experiments in a laboratory setting, and various assumptions must be examined to apply this result to the dynamics of radiocesium under natural conditions of forest soils. In this study, we used a simple and relatively high-concentration CsCl solution to estimate how much radiocesium in the initial throughfall can be sorbed. Although we examined the impact of pH in the solution by using pH standard buffer solutions, ion strength and other competing ions (potassium in particular) in the solution also are expected to affect Cs sorption [9, 10, 22, 35]. The carrier effect of radiocesium with a significantly low concentration in molar units should be considered [24].

In addition, to homogenize each sample, we mixed and powdered them before analysis. We used a reciprocating shaker for up to 48 h to complete Cs sorption uniformly on each sample. However, in the natural condition, organic matter is bulky and heterogeneous. Koarashi et al. [19] reported different amounts of Cs retention in different organic matter sizes. Contact of throughfall with organic matter in forest

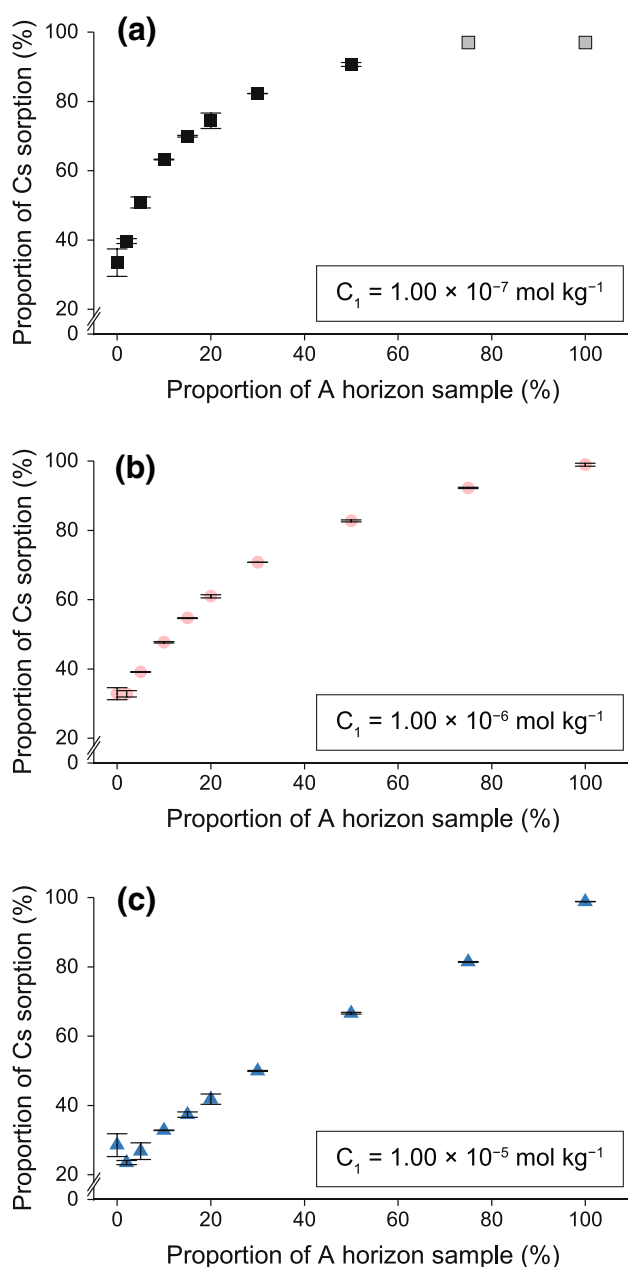


Fig. 4 Scatter plots of the proportion (%) of Cs sorption and the mass of the A horizon sample in the mixture with needles as organic matter. Three Cs concentrations are shown: initial solution (C_1) of **a** 1.00×10^{-7} , **b** 1.00×10^{-6} , and **c** 1.00×10^{-5} mol kg^{-1} in Experiment A-2. The data for the proportion of the A horizon sample being 0 and 100% were obtained in Experiment A (shown in Fig. 1 and Table 2). The error bars indicate 1 SD. In the condition $C_1 = 1.00 \times 10^{-7}$ mol kg^{-1} , for some samples, Cs concentration of the filtrates (C_2) was lower than the method quantification limit (3×10^{-9} mol kg^{-1}). For such cases, we set the proportion of Cs sorption as 97% and plotted them as gray squares

soils is also complicated; both infiltration and interception function of water are observed in the O horizon [49], resulting in heterogeneous radiocesium sorption. For these

reasons, further studies with different methods or samples are required to recognize radiocesium cycling in forest ecosystems more accurately.

Mobility and bioavailability of cesium sorbed by each sample

By using Q_{0-B} and C_3 values, we calculated the proportion of Cs desorption (%) by ultrapure water or ammonium acetate with the following equation:

$$\text{Proportion of Cs desorption (\%)} = (C_3 M_{\text{solution}}) / (Q_{0-B} M_{\text{sample}}) \times 100 \quad (5)$$

Figure 5 summarizes the results. Some samples show higher ($C_3 M_{\text{solution}}$) values than ($Q_{0-B} M_{\text{sample}}$) values for ammonium acetate, perhaps due to analytical errors (e.g., for the cellulose powder, ($C_3 M_{\text{solution}}$) and ($Q_{0-B} M_{\text{sample}}$) values were calculated to be 2.66×10^{-8} and 2.52×10^{-8} mol, respectively). For these samples, we set the proportion of Cs desorption to 100%.

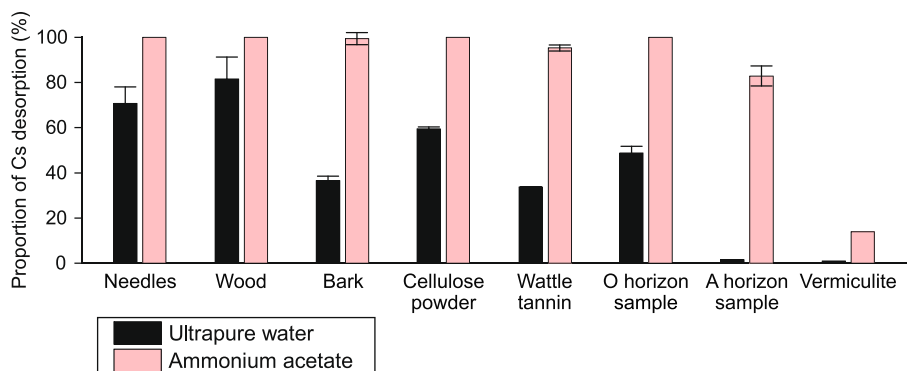
For organic matter samples, ultrapure water and ammonium acetate extracted approximately 37%–82% and almost all of the sorbed Cs, respectively (Fig. 5). This suggests that the Cs sorbed on fresh plant residues was relatively mobile; thus, fresh plant residues can only work as temporary reservoirs of Cs in the Oi horizon.

This phenomenon also has been demonstrated in the natural condition. For example, Sakai et al. [50] soaked fresh litter with stream water and found that a great amount of radiocesium that was originally sorbed in the litter was easily washed out. In stem wood, Cs is easily redistributed by the movement of free water [51][51]. Aoki et al. [53] conducted a Cs sorption experiment on wood powder and examined the absorption fine structure by X-ray analysis. They concluded that Cs in the wood forms an outer-sphere complex in a hydrated state. With bark, although our Experiment A demonstrated high Cs sorption, Cs absorption by trees through bark has been reported [39, 54]. Therefore, Cs sorbed by bark also may be mobile.

As expected, vermiculite demonstrated a relatively low proportion of Cs desorption (Fig. 5). As proposed in previous studies, Cs forms an inner-sphere complex with FES and type II sites in vermiculite with strong affinity and is scarcely extractable [7–11].

The results of this laboratory study can only be cautiously applied to the natural condition of forest soils. In our O horizon sample, the proportion of Cs desorption was the same level as that of organic matter samples (Fig. 5). The A horizon sample demonstrated a relatively low proportion for ultrapure water, but ammonium acetate extracted as much as 83% of sorbed Cs (Fig. 5). However, in the natural condition, the proportion of water and

Fig. 5 Bar charts of the proportion (%) of Cs desorption by ultrapure water (black) or ammonium acetate (red) (Experiment B). The error bars indicate 1 SD. For some samples showing higher (C_3 M_{solution}) values than (Q_{0-B} M_{sample}) values, we set the proportion of Cs desorption to 100%



ammonium acetate-extractable ^{137}Cs is very low: less than 4% and 27%, respectively [6, 55, 56].

These differences are likely caused by the different conditions of our desorption experiments compared with the natural conditions of forest soils. As shown in our Experiment A-2, we used homogenized samples and high-concentration Cs solutions compared with radiocesium under natural conditions. In the process of Cs sorption and residue recovery prior to Experiment B, it was not possible to recover the Cs solution completely from the residue via the suction filtration process. Nevertheless, the residue that was recovered was dried without washing and used in Experiment B. Therefore, we may have overestimated the proportion of Cs desorption. Chemical alteration of organic matter may also occur in the drying process. In contrast, under natural conditions, a special accumulation of ^{137}Cs on organic matter also was reported via size and density fractionation methods [12, 57] and chemical sequential fractionation methods [13]. Biological absorption of radiocesium also should occur. Hara et al. [58] suggested the incorporation of ^{137}Cs into the fine structure of plant tissues and reported the existence of ammonium acetate-insoluble ^{137}Cs in Japanese cedar needles. By considering the transfer of these leaves/needles onto the forest floor via litterfall, radiocesium in the O horizon should be more immobile compared with our assumption on Cs. In addition, microorganisms such as fungi can alter radiocesium forms [59–61]. Furthermore, for the A horizon sample, Takeda et al. [24] proposed that aging and drying–wetting cycles can stimulate Cs fixation by clay minerals.

For these reasons, further studies are needed to recognize a more accurate picture of radiocesium cycling in forest ecosystems. However, as a first trial, our experiments suggest that, regardless of the types of fresh plant residues in the Oi horizon, a large part of the sorbed radiocesium may rapidly migrate downward or be easily taken up by plant roots or microorganisms.

Conclusions

We conducted sorption and desorption experiments with Cs solution on various organic matter samples to estimate the radiocesium sorption characteristics of individual fresh plant residues in the Oi horizon. The Cs sorption of all our samples was described by the Freundlich isotherm model. Among the samples tested herein, bark and wattle tannin sorbed a relatively large amount of Cs. This sorption is likely controlled by pH-dependent negative charges, such as phenolic hydroxyl or carboxyl groups on these samples. In contrast, samples containing clay minerals showed much higher Cs sorption. Sorption experiments for mixtures of cedar needles and A horizon samples revealed that the proportion of Cs sorption drastically increased with even small incorporation of clay minerals, particularly with lower Cs concentrations. For the desorption experiments, a large part of sorbed Cs was easily extracted by ultrapure water or ammonium acetate, suggesting that the Cs sorbed by fresh plant residues is relatively mobile. Although our experiments were simple trials conducted in a laboratory setting and further studies are needed before applying these results to the radiocesium dynamics in the natural conditions of forests in Fukushima (e.g., the chemical composition of the solution, biological absorption of Cs), our results suggest that fresh plant residues can only work as temporary reservoirs of radiocesium in the Oi horizon.

Appendix

See Tables 2 and 3.

Acknowledgements We thank the village office of Kawauchi and the Kanto Regional Forest Office of the Forestry Agency for their permission to conduct field investigations. Our special thanks to Dr. M. Komatsu (Forestry and Forest Products Research Institute) for support with sample preparation. We also are grateful to many researchers and staff members of the Forestry and Forest Products Research Institute

Table 2 Initial concentration of CsCl solution (C_1) and Cs concentration of the filtrates (C_2) for each contact time in Experiment A. For wattle tannin, only 24 h shaking was conducted

Initial concentration of CsCl solution (C_1) (mol kg ⁻¹)	Cs concentration of the filtrates (C_2) (mol kg ⁻¹)							
	Needles	Wood	Bark	Cellulose powder	Wattle tannin	O horizon sample	A horizon sample	Vermiculite
<i>Contact time: 2 h</i>								
1.00×10^{-7}	7.4×10^{-8}	8.2×10^{-8}	6.0×10^{-8}	7.9×10^{-8}	–	4.1×10^{-8}	$< 0.3 \times 10^{-8}$	$< 0.3 \times 10^{-8}$
1.00×10^{-6}	7.6×10^{-7}	8.2×10^{-7}	6.1×10^{-7}	7.8×10^{-7}	–	4.9×10^{-7}	0.32×10^{-7}	0.067×10^{-7}
1.00×10^{-5}	8.0×10^{-6}	8.6×10^{-6}	6.3×10^{-6}	8.2×10^{-6}	–	5.2×10^{-6}	0.58×10^{-6}	0.10×10^{-6}
1.00×10^{-4}	8.1×10^{-5}	8.5×10^{-5}	6.5×10^{-5}	8.0×10^{-5}	–	5.5×10^{-5}	1.4×10^{-5}	0.22×10^{-5}
1.00×10^{-3}	7.9×10^{-4}	8.4×10^{-4}	6.9×10^{-4}	8.6×10^{-4}	–	6.1×10^{-4}	5.1×10^{-4}	0.55×10^{-4}
<i>Contact time: 24 h</i>								
1.00×10^{-7}	6.7×10^{-8}	8.0×10^{-8}	6.0×10^{-8}	7.2×10^{-8}	3.9×10^{-8}	3.8×10^{-8}	$< 0.3 \times 10^{-8}$	$< 0.3 \times 10^{-8}$
1.00×10^{-6}	6.7×10^{-7}	7.6×10^{-7}	6.1×10^{-7}	7.2×10^{-7}	3.5×10^{-7}	5.0×10^{-7}	0.20×10^{-7}	0.11×10^{-7}
1.00×10^{-5}	7.1×10^{-6}	8.0×10^{-6}	6.4×10^{-6}	7.4×10^{-6}	3.0×10^{-6}	5.2×10^{-6}	0.54×10^{-6}	0.12×10^{-6}
1.00×10^{-4}	7.3×10^{-5}	7.8×10^{-5}	6.4×10^{-5}	7.5×10^{-5}	3.8×10^{-5}	5.5×10^{-5}	1.2×10^{-5}	0.23×10^{-5}
1.00×10^{-3}	7.8×10^{-4}	8.3×10^{-4}	7.4×10^{-4}	8.8×10^{-4}	5.1×10^{-4}	6.5×10^{-4}	4.5×10^{-4}	0.43×10^{-4}
<i>Contact time: 48 h</i>								
1.00×10^{-7}	7.3×10^{-8}	8.1×10^{-8}	6.0×10^{-8}	7.6×10^{-8}	–	3.9×10^{-8}	$< 0.3 \times 10^{-8}$	$< 0.3 \times 10^{-8}$
1.00×10^{-6}	7.5×10^{-7}	8.0×10^{-7}	6.1×10^{-7}	7.6×10^{-7}	–	5.0×10^{-7}	0.19×10^{-7}	0.10×10^{-7}
1.00×10^{-5}	7.7×10^{-6}	8.1×10^{-6}	6.4×10^{-6}	7.6×10^{-6}	–	5.3×10^{-6}	0.44×10^{-6}	0.12×10^{-6}
1.00×10^{-4}	7.9×10^{-5}	8.2×10^{-5}	6.6×10^{-5}	7.6×10^{-5}	–	5.8×10^{-5}	1.1×10^{-5}	0.24×10^{-5}
1.00×10^{-3}	7.8×10^{-4}	8.6×10^{-4}	7.3×10^{-4}	8.6×10^{-4}	–	6.5×10^{-4}	4.3×10^{-4}	0.46×10^{-4}

Table 3 Parameters for the Freundlich isotherm model (Eq. 4) for each contact time for each sample in Experiment A. Data that were lower than the method quantification limit (Table 2) were not used for this calculation

Component	Equation: $\log Q_1 = \log K_f + 1/n \log C_2$								
	Contact time: 2 h			Contact time: 24 h			Contact time: 48 h		
	1/n	$\log K_f$	r^2	1/n	$\log K_f$	r^2	1/n	$\log K_f$	r^2
Needles	0.96	0.55	0.999	0.94	0.59	1.000	0.97	0.63	1.000
Wood	0.98	0.47	0.999	0.98	0.61	0.998	0.96	0.46	0.999
Bark	0.96	0.85	1.000	0.94	0.73	0.999	0.94	0.73	0.999
Cellulose powder	0.95	0.40	0.999	0.90	0.27	0.994	0.94	0.42	0.996
Wattle tannin	–	–	–	0.95	1.24	0.994	–	–	–
O horizon sample	0.92	0.85	1.000	0.90	0.75	0.999	0.90	0.71	1.000
A horizon sample	0.65	0.23	0.988	0.64	0.25	0.994	0.64	0.28	0.994
Vermiculite	0.76	1.54	0.998	0.82	1.89	0.998	0.81	1.83	0.999

for their support with experiments. This work was supported by JSPS KAKENHI (Grant Number 18K14495).

Open Access This article is licensed under a Creative Commons Attribution 4.0 International License, which permits use, sharing, adaptation, distribution and reproduction in any medium or format, as long as you give appropriate credit to the original author(s) and the source, provide a link to the Creative Commons licence, and indicate if changes were made. The images or other third party material in this article are included in the article's Creative Commons licence, unless indicated otherwise in a credit line to the material. If material is not included in the article's Creative Commons licence and your intended use is not permitted by statutory regulation or exceeds the permitted use, you will

need to obtain permission directly from the copyright holder. To view a copy of this licence, visit <http://creativecommons.org/licenses/by/4.0/>.

References

- Katata G, Ota M, Terada H et al (2012) Atmospheric discharge and dispersion of radionuclides during the Fukushima Dai-ichi Nuclear Power Plant accident. Part I: Source term estimation and local-scale atmospheric dispersion in early phase of the accident. *J Environ Radioact* 109:103–113. <https://doi.org/10.1016/j.jenvrad.2012.02.006>

2. Terada H, Katata G, Chino M, Nagai H (2012) Atmospheric discharge and dispersion of radionuclides during the Fukushima Dai-ichi Nuclear Power Plant accident. Part II: verification of the source term and analysis of regional-scale atmospheric dispersion. *J Environ Radioact* 112:141–154. <https://doi.org/10.1016/j.jenvrad.2012.05.023>
3. Nakajima T, Misawa S, Morino Y et al (2017) Model depiction of the atmospheric flows of radioactive cesium emitted from the Fukushima Daiichi Nuclear Power Station accident. *Prog Earth Planet Sci* 4:2. <https://doi.org/10.1186/s40645-017-0117-x>
4. Nishikiori T, Watanabe M, Koshikawa MK et al (2019) ^{137}Cs transfer from canopies onto forest floors at Mount Tsukuba in the four years following the Fukushima nuclear accident. *Sci Total Environ* 659:783–789. <https://doi.org/10.1016/j.scitotenv.2018.12.359>
5. Kato H, Onda Y, Hisadome K et al (2017) Temporal changes in radiocesium deposition in various forest stands following the Fukushima Dai-ichi Nuclear Power Plant accident. *J Environ Radioact* 166:449–457. <https://doi.org/10.1016/j.jenvrad.2015.04.016>
6. Manaka T, Imamura N, Kaneko S et al (2019) Six-year trends in exchangeable radiocesium in Fukushima forest soils. *J Environ Radioact* 203:84–92. <https://doi.org/10.1016/j.jenvrad.2019.02.014>
7. Cremers A, Elsen A, Preter P De, Maes A (1988) Quantitative analysis of radiocesium retention in soils. *Nature* 335:247–249. <https://doi.org/10.1038/335247a0>
8. Bradbury MH, Baeyens B (2000) A generalised sorption model for the concentration dependent uptake of caesium by argillaceous rocks. *J Contam Hydrol* 42:141–163. [https://doi.org/10.1016/S0169-7722\(99\)00094-7](https://doi.org/10.1016/S0169-7722(99)00094-7)
9. Fuller AJ, Shaw S, Peacock CL et al (2014) Ionic strength and pH dependent multi-site sorption of Cs onto a micaceous aquifer sediment. *Appl Geochemistry* 40:32–42. <https://doi.org/10.1016/j.apgeochem.2013.10.017>
10. Fan QH, Tanaka M, Tanaka K et al (2014) An EXAFS study on the effects of natural organic matter and the expandability of clay minerals on cesium adsorption and mobility. *Geochim Cosmochim Acta* 135:49–65. <https://doi.org/10.1016/j.gca.2014.02.049>
11. Okumura M, Kerisit S, Bourg IC et al (2018) Radiocesium interaction with clay minerals: theory and simulation advances Post-Fukushima. *J Environ Radioact* 189:135–145. <https://doi.org/10.1016/j.jenvrad.2018.03.011>
12. Koarashi J, Nishimura S, Atarashi-Andoh M et al (2019) A new perspective on the ^{137}Cs retention mechanism in surface soils during the early stage after the Fukushima nuclear accident. *Sci Rep* 9:7034. <https://doi.org/10.1038/s41598-019-43499-7>
13. Manaka T, Ono K, Furusawa H et al (2020) Chemical sequential extraction of O horizon samples from Fukushima forests: assessment for degradability and radiocesium retention capacity of organic matters. *J Environ Radioact* 220–221:106306. <https://doi.org/10.1016/j.jenvrad.2020.106306>
14. Kruyts N, Delvaux B (2002) Soil organic horizons as a major source for radiocesium biorecycling in forest ecosystems. *J Environ Radioact* 58:175–190. [https://doi.org/10.1016/S0265-931X\(01\)00065-0](https://doi.org/10.1016/S0265-931X(01)00065-0)
15. Dumat C, Staunton S (1999) Reduced adsorption of caesium on clay minerals caused by various humic substances. *J Environ Radioact* 46:187–200. [https://doi.org/10.1016/S0265-931X\(98\)00125-8](https://doi.org/10.1016/S0265-931X(98)00125-8)
16. Dumat C, Quiquampoix H, Staunton S (2000) Adsorption of cesium by synthetic clay–organic matter complexes: effect of the nature of organic polymers. *Environ Sci Technol* 34:2985–2989. <https://doi.org/10.1021/es990657o>
17. Tashiro Y, Nakao A, Wagai R et al (2018) Inhibition of radiocesium adsorption on 2:1 clay minerals under acidic soil environment: effect of organic matter vs. hydroxy aluminum polymer. *Geoderma* 319:52–60. <https://doi.org/10.1016/j.geoderma.2017.12.039>
18. Tatsuno T, Hamamoto S, Nihei N, Nishimura T (2020) Effects of the dissolved organic matter on Cs transport in the weathered granite soil. *J Environ Manage* 254:109785. <https://doi.org/10.1016/j.jenvman.2019.109785>
19. Koarashi J, Atarashi-Andoh M, Takeuchi E, Nishimura S (2014) Topographic heterogeneity effect on the accumulation of Fukushima-derived radiocesium on forest floor driven by biologically mediated processes. *Sci Rep*. <https://doi.org/10.1038/srep06853>
20. Kurihara M, Onda Y, Suzuki H et al (2018) Spatial and temporal variation in vertical migration of dissolved ^{137}Cs passed through the litter layer in Fukushima forests. *J Environ Radioact* 192:1–9. <https://doi.org/10.1016/j.jenvrad.2018.05.012>
21. Mimura H, Kanno T (1985) Distribution and fixation of cesium and strontium in zeolite A and chabazite. *J Nucl Sci Technol* 22:284–291. <https://doi.org/10.3327/jnst.22.284>
22. Yamauchi S, Yamagishi T, Kirikoshi K, Yatagai M (2014) Cesium adsorption from aqueous solutions onto Japanese oak charcoal I: effects of the presence of group 1 and 2 metal ions. *J Wood Sci* 60:473–479. <https://doi.org/10.1007/s10086-014-1431-1>
23. Shao H, Wei Y, Li F (2019) Fixation capability of recycling materials as potential additives for cesium immobilization in contaminated forest soil. *J Radioanal Nucl Chem* 319:315–326. <https://doi.org/10.1007/s10967-018-6353-8>
24. Takeda A, Tsukada H, Nakao A et al (2013) Time-dependent changes of phytoavailability of Cs added to allophanic Andosols in laboratory cultivations and extraction tests. *J Environ Radioact* 122:29–36. <https://doi.org/10.1016/j.jenvrad.2013.02.005>
25. Imamura N, Komatsu M, Ohashi S et al (2017) Temporal changes in the radiocesium distribution in forests over the five years after the Fukushima Daiichi Nuclear power plant accident. *Sci Rep* 7:8179. <https://doi.org/10.1038/s41598-017-08261-x>
26. Takeda A, Tsukada H, Takaku Y et al (2006) Extractability of major and trace elements from agricultural soils using chemical extraction methods: application for phytoavailability assessment. *Soil Sci Plant Nutr* 52:406–417. <https://doi.org/10.1111/j.1747-0765.2006.00066.x>
27. Inagaki Y, Inagaki M, Hashimoto T, et al (2012) Aboveground production and nitrogen utilization in nitrogen-saturated coniferous plantation forests on the periphery of the Kanto Plain. *Bull FFPRI* 11:161–173. <https://www.ffpri.affrc.go.jp/pubs/bulletin/424/documents/424-6.pdf>
28. IUSS Working Group WRB (2015) World Reference Base for Soil Resources 2014, update 2015, International soil classification system for naming soils and creating legends for soil maps. Rome
29. Forestry Agency of Japan (2014) Preliminary results of surveys of radioactive element distribution in forest ecosystems in fiscal year 2013. <https://www.rinya.maff.go.jp/j/kouhou/jisin/attach/pdf/H27izen-5.pdf>. Accessed 15 Jan 2021 (in Japanese)
30. Ikeda S, Kaneko S, Akama A, Takahashi M (2014) Methods for assessing the spatial distribution and dynamics of radiocesium in forest soils. *Bull FFPRI* 13:137–145. <http://www.ffpri.affrc.go.jp/pubs/bulletin/432/documents/432-6.pdf> (in Japanese with English abstract)
31. Ogata T, Kim YH, Nakano Y (2007) Selective recovery process for gold utilizing a functional gel derived from natural condensed Tannin. *J Chem Eng JAPAN* 40:270–274. <https://doi.org/10.1252/cej.40.270>
32. Carter MR, Gregorich EG (2007) Soil sampling and methods of analysis. CRC Press, Boca Raton, FL, Second Edition
33. Miura A, Kubota T, Hamada K, Hitomi T (2016) Adsorption efficiency of natural materials for low-concentration cesium in

- solution. *Water Sci Technol* 73:2453–2460. <https://doi.org/10.2166/wst.2016.098>
34. Slabbert N (1992) Complexation of condensed tannins with metal ions. In: Hemingway RW, Laks PE (eds) *Plant polyphenols: synthesis, properties, significance*. Springer, US, Boston, MA, pp 421–436. https://doi.org/10.1007/978-1-4615-3476-1_23
 35. Lofts S, Tipping EW, Sanchez AL, Dodd BA (2002) Modelling the role of humic acid in radiocaesium distribution in a British upland peat soil. *J Environ Radioact* 61:133–147. [https://doi.org/10.1016/S0265-931X\(01\)00118-7](https://doi.org/10.1016/S0265-931X(01)00118-7)
 36. Kanô F, Abe I, Kamaya H, Ueda I (2000) Fractal model for adsorption on activated carbon surfaces: Langmuir and Freundlich adsorption. *Surf Sci* 467:131–138. [https://doi.org/10.1016/S0039-6028\(00\)00730-5](https://doi.org/10.1016/S0039-6028(00)00730-5)
 37. Ebato M, Yonebayashi K (2004) Identification of adsorption conditions fulfilling the correlation between freundlich isotherm coefficients, $\log K_F$ and $1/n$ by computer simulation. *Soil Sci Plant Nutr* 50:171–179. <https://doi.org/10.1080/00380768.2004.10408466>
 38. Su P, Granholm K, Pranovich A et al (2013) Sorption of metal ions from aqueous solution to spruce bark. *Wood Sci Technol* 47:1083–1097. <https://doi.org/10.1007/s00226-013-0562-7>
 39. Wang W, Takenaka C, Tomioka R, Kanasashi T (2018) Absorption and translocation of cesium through Konara oak (*Quercus serrata*) bark. *J For Res* 23:35–40. <https://doi.org/10.1080/13416979.2018.1426898>
 40. Ono K, Hiradate S, Morita S et al (2011) Humification processes of needle litters on forest floors in Japanese cedar (*Cryptomeria japonica*) and Hinoki cypress (*Chamaecyparis obtusa*) plantations in Japan. *Plant Soil* 338:171–181. <https://doi.org/10.1007/s11104-010-0397-z>
 41. Celebi O, Kilikli A, Erten HN (2009) Sorption of radioactive cesium and barium ions onto solid humic acid. *J Hazard Mater* 168:695–703. <https://doi.org/10.1016/j.jhazmat.2009.02.090>
 42. Zhang C, Su J, Zhu H et al (2017) The removal of heavy metal ions from aqueous solutions by amine functionalized cellulose pretreated with microwave-H₂O₂. *RSC Adv* 7:34182–34191. <https://doi.org/10.1039/C7RA03056H>
 43. Burger A, Lichtscheidl I (2018) Stable and radioactive cesium: A review about distribution in the environment, uptake and translocation in plants, plant reactions and plants' potential for bioremediation. *Sci Total Environ* 618:1459–1485. <https://doi.org/10.1016/j.scitotenv.2017.09.298>
 44. Morimoto K, Tamura K, Umemura Y et al (2011) Capture of radioactive nuclear wastes from sea water by use of clay minerals. *Chem Lett* 40:867–869. <https://doi.org/10.1246/cl.2011.867>
 45. Morimoto K, Kogure T, Tamura K et al (2012) Desorption of Cs⁺ ions intercalated in vermiculite clay through cation exchange with Mg²⁺ ions. *Chem Lett* 41:1715–1717. <https://doi.org/10.1246/cl.2012.1715>
 46. Fujii K, Yamaguchi N, Imamura N et al (2019) Effects of radiocaesium fixation potentials on ¹³⁷Cs retention in volcanic soil profiles of Fukushima forests. *J Environ Radioact* 198:126–134. <https://doi.org/10.1016/j.jenvrad.2018.12.025>
 47. Wauters J, Elsen A, Cremers A et al (1996) Prediction of solid/liquid distribution coefficients of radiocaesium in soils and sediments. Part one: a simplified procedure for the solid phase characterisation. *Appl Geochemistry* 11:589–594. [https://doi.org/10.1016/0883-2927\(96\)00027-3](https://doi.org/10.1016/0883-2927(96)00027-3)
 48. Povinec PP, Hirose K, Aoyama M (2013) Fukushima accident. Elsevier, Amsterdam, Netherlands. <https://doi.org/10.1016/C2012-0-06837-8>
 49. Sato Y, Kumagai T, Kume A et al (2004) Experimental analysis of moisture dynamics of litter layers?—the effects of rainfall conditions and leaf shapes. *Hydrol Process* 18:3007–3018. <https://doi.org/10.1002/hyp.5746>
 50. Sakai M, Gomi T, Naito RS et al (2015) Radiocaesium leaching from contaminated litter in forest streams. *J Environ Radioact* 144:15–20. <https://doi.org/10.1016/j.jenvrad.2015.03.001>
 51. Brown GN (1964) Cesium in lirioidendron and other woody species: organic bonding sites. *Science* (80-) 143:368–369. <https://doi.org/10.1126/science.143.3604.368>
 52. Tanaka T, Murakami K, Kumata A, Kawai Y (2015) Influence of drying temperature on the migration of cesium chloride initially dissolved in the liquid water of sugi (*Cryptomeria japonica* D. Don) sapwood. *Wood Sci Technol* 49:915–924. <https://doi.org/10.1007/s00226-015-0746-4>
 53. Aoki D, Asai R, Tomioka R et al (2017) Translocation of ¹³³Cs administered to *Cryptomeria japonica* wood. *Sci Total Environ* 584–585:88–95. <https://doi.org/10.1016/j.scitotenv.2017.01.159>
 54. Wang W, Hanai Y, Takenaka C et al (2016) Cesium absorption through bark of Japanese cedar (*Cryptomeria japonica*). *J For Res* 21:251–258. <https://doi.org/10.1007/s10310-016-0534-5>
 55. Matsunaga T, Koarashi J, Atarashi-Andoh M et al (2013) Comparison of the vertical distributions of Fukushima nuclear accident radiocaesium in soil before and after the first rainy season, with physicochemical and mineralogical interpretations. *Sci Total Environ* 447:301–314. <https://doi.org/10.1016/j.scitotenv.2012.12.087>
 56. Saito T, Makino H, Tanaka S (2014) Geochemical and grain-size distribution of radioactive and stable cesium in Fukushima soils: Implications for their long-term behavior. *J Environ Radioact* 138:11–18. <https://doi.org/10.1016/j.jenvrad.2014.07.025>
 57. Toriyama J, Kobayashi M, Hiruta T, Shichi K (2018) Distribution of radiocaesium in different density fractions of temperate forest soils in Fukushima. *For Ecol Manage* 409:260–266. <https://doi.org/10.1016/j.foreco.2017.11.024>
 58. Hara T, Takenaka C, Tomioka R (2020) Change in the chemical form of ¹³⁷Cs with age in needles of Japanese cedar. *J Environ Radioact* 213:106137. <https://doi.org/10.1016/j.jenvrad.2019.106137>
 59. Steiner M, Linkov I, Yoshida S (2002) The role of fungi in the transfer and cycling of radionuclides in forest ecosystems. *J Environ Radioact* 58:217–241. [https://doi.org/10.1016/S0265-931X\(01\)00067-4](https://doi.org/10.1016/S0265-931X(01)00067-4)
 60. Vinichuk MM, Johanson KJ, Rosén K, Nilsson I (2005) Role of the fungal mycelium in the retention of radiocaesium in forest soils. *J Environ Radioact* 78:77–92. <https://doi.org/10.1016/j.jenvrad.2004.02.008>
 61. Ogo S, Yamanaka T, Akama K et al (2018) Influence of ectomycorrhizal colonization on cesium uptake by *Pinus densiflora* seedlings. *Mycobiology* 46:388–395. <https://doi.org/10.1080/12298093.2018.1538074>

Publisher's Note Springer Nature remains neutral with regard to jurisdictional claims in published maps and institutional affiliations.